



STRUCTURAL, OPTICAL, ELECTRICAL AND THERMAL PROPERTIES OF InP CRYSTALS

M. P. DESHPANDE¹, HITESHKUMAR R. BHOI², KIRAN N. PATEL, PIYUSH RAJPUT, KRISHNABEN CHAUHAN,
S. H. CHAKI AND ANKUR J. KHIMANI

Department of Physics, Sardar Patel University, Vallabh Vidyanagar, Anand, 38120 Gujarat, India.

Email: vishwadeshpande@yahoo.co.in¹, bhoihitesh92@live.com²

ABSTRACT

The structural, optical, electrical and thermal properties of as grown Indium Phosphide crystals (InP) are investigated in this present work. The crystals provided to us were grown by Liquid Encapsulated Czochralski (LEC) method. We have used this crystal to characterize and study the various properties of it. The EDAX spectra showed the purity of given crystals. The structural parameters are calculated from the Powder X-ray Diffractogram (XRD). The band gap of crystal was determined from UV-VIS-NIR spectra. Raman spectra was obtained in the temperature range 80K to 300K from which Gruneisen parameter and isobaric Raman shift were calculated. Resistivity showed the semiconducting nature of InP crystals and we measured thermal conductivity at 80°C temperature. Hall-effect measurement and Thermoelectric power measurements showed the n-type nature of this crystal.

Keywords: InP Crystal, Raman spectroscopy, isobaric Raman shift

1. INTRODUCTION

InP is an important material due to its excellent optical properties. Therefore, the study of InP crystals is very significant. InP is III-V compound semiconductor with n-type behavior. InP has a face centered cubic “Zinc blende” structure. InP has been extensively investigated recently for various scientific and technological aspects and to excess new class of fundamental material for high speed semiconductor technology. InP is a key material for opto-electronics and finds application in different optical and microwave devices. InP as a substrate material provides good thermal stability and crystal perfection in semiconductor technology [1].

In the present article, we report the structural, optical, electrical and thermal properties of InP crystals by various characterization techniques.

2. METHODOLOGY

We have used here InP crystals grown by Liquid Encapsulated Czochralski (LEC) method provided to us by other worker.

3. OBSERVATIONS

The elemental composition of given InP samples was determined by energy dispersive analysis of

X-rays (EDAX) attached with Philips EM400 electron microscope. X-ray diffraction pattern of powdered InP crystal was recorded on Rigaku X-ray diffractometer with $\text{CuK}\alpha$ radiation ($\lambda=1.5418 \text{ \AA}$). Energy gap of InP crystal was measured by UV-VIS-NIR Perkin Elmer Lambda 19 (Range: 180-3200 nm) spectrometer. Room temperature Raman spectra is obtained with the help of Jobin Yvon Horibra LABRAM-HR visible (400 – 1100 nm) with diode laser (473nm, 25mW) as an excitation source. Low temperature Raman spectra of InP crystals was also obtained with the same instrument in the temperature range (80 K – 260 K). For variable temperature measurement there is a LINKAM THMS 600 heating and cooling microscope stage, which allows for the micro-Raman measurement to be performed within 77K to 900K temperature range.

Temperature dependent resistivity of sample is measured with increasing temperature. The sample is sandwiched between two holders having resistance measuring probe. The sample thickness and surface area are measured in prior to the experiment performed then the value of resistivity is determined. The resistance of the sample is measured directly with RISH multi 12S unit, the sample assembly is inserted into the

furnace and measurements are recorded at a difference of 5°C.

The thermal conductivity of the crystal was measured by the simplest method known as divided bar method [2]. The temperature of the furnace is controlled with dimmerstat. In this method a thin crystal plate whose thermal conductivity is to be measured is sandwiched between two metal rods. The cross section of crystal was of same size of that metal sample holder. The heat is provided from the one end of metal rod passing through the crystal and finally out from the second metal rod. Conditions are controlled so that a steady state is reached.

For Hall-effect measurement the experiment was performed using Hall-effect setup, electrical contacts are taken by silver paste and connected to Hall probe. The results were measured keeping constant magnetic field of 1000 gauss and 1500 gauss, then varying the probe current, Hall voltages are measured.

The Seebeck coefficient, also known as the thermoelectric power or thermo-power, is usually measured by a dc or ac technique [3]. Here, we have discussed dc technique which is one of the simplest transport measurements. It requires a thermal gradient to be established along a sample and measuring both the thermoelectric voltage and the temperature difference between two points along the length of the sample. The Seebeck coefficient is then simply obtained by simple relation.

4. RESULTS AND DISCUSSION

4.1 Elemental analysis

EDAX analysis: It is evident from EDAX spectra that no elemental peaks other than In and P were observed indicating purity of grown crystals as shown in **figure 4.1**

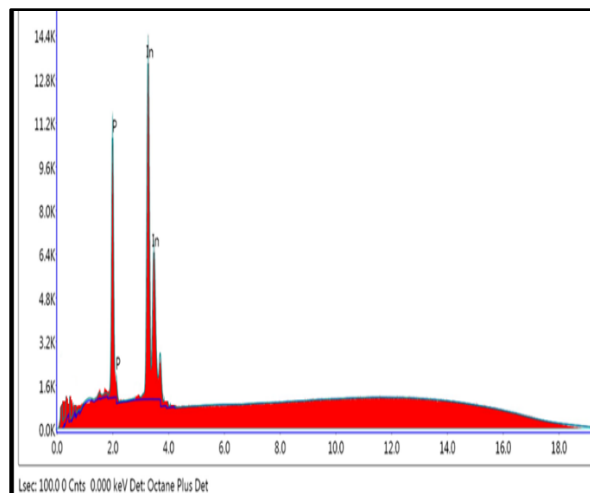


Figure 4.1 EDAX spectra of InP crystal

The weight percentage of In and P comes out as 48.30 and 51.70 respectively which matches with reported value [4].

4.2 Structural property

X-ray diffraction (XRD) study: The X-ray diffractogram is shown in **figure 4.2**.

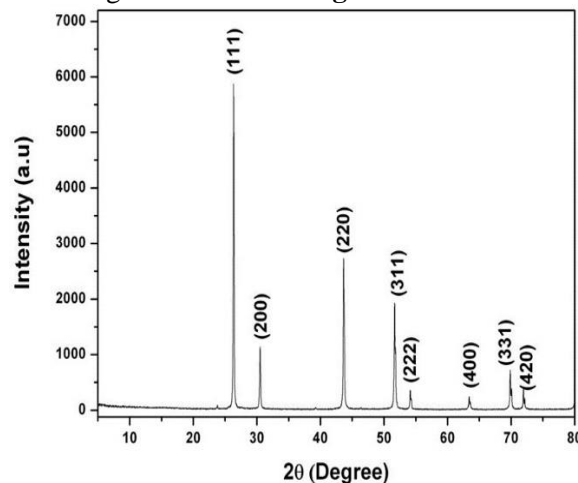


Figure 4.2 X-ray Diffractogram

The peak appearing at $2\theta = 26.36^\circ, 30.52^\circ, 43.66^\circ, 51.69^\circ, 54.16^\circ, 63.40^\circ, 69.86^\circ$ and 71.93° are indexed as (111), (200), (220), (311), (222), (400), (331) and (420) respectively based on a Zinc blend structure of InP with B3 phase (JCPDS file no. 10-0216) [4]. The lattice parameter comes out to be 5.860\AA which is very

close to reported value. Also the crystalite size of InP crystals varies from 62.45nm to 94.67nm.

4.3 Optical studies

4.3.1 UV-VIS-NIR spectroscopy: The UV-VIS-NIR absorption spectra of InP crystal appears at around 840 nm. We have determined the energy band gap of InP crystals using well known Tauc relation [5].

$$(\alpha h\nu)^n = A (h\nu - E_g) \quad (1)$$

where, α is the absorption coefficient, $h\nu$ is photon energy, A is absorbance, E_g is optical band gap, n is the number characterising the nature of the transition process, $n=2$ for the direct transition and $n=1/2$ for indirect transition. Hence, the optical band gap for the absorption edge can be obtained by extrapolating the linear portion of the $(\alpha h\nu)^n$ Vs. $h\nu$ curve to the energy axis as shown in **figure 4.3**.

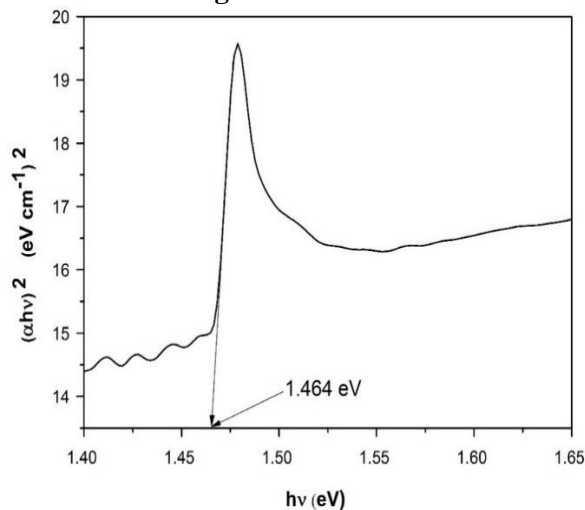


Figure 4.3 Tauc plot of InP crystal

The band gap energy estimated from Tauc plot comes out to be 1.46 eV and matches well with the reported value 1.41 eV [6].

4.3.2 Raman Spectroscopy: Results from Raman spectroscopy shows presence of TO mode at 300.2 cm^{-1} and LO mode at 339.1 cm^{-1} at room temperature [7]. Further, the measurement at liquid nitrogen (80 K) temperature shows TO at 306.81 cm^{-1} and LO at 344.87 cm^{-1} [8,9].

Low temperature Raman spectra of InP was also studied in the temperature range (80 K – 260 K). Raman peak are found to increase with decrease in temperature. Furthermore, in these temperature range line width are continuous and gradual down to 80 K. The plot of intensity Vs Raman shift is displayed in the **figure 4.4** at different temperatures. It can be seen that as temperature decreases the Raman peak for both TO and LO mode becomes sharper and shifts towards right hand side. The change in Raman spectra in this temperature range are related to change in strength of bond due to the temperature induced lattice volume expansion. The temperature dependent Raman shift in peaks shows thermal expansion and anharmonic interaction between the phonon modes.

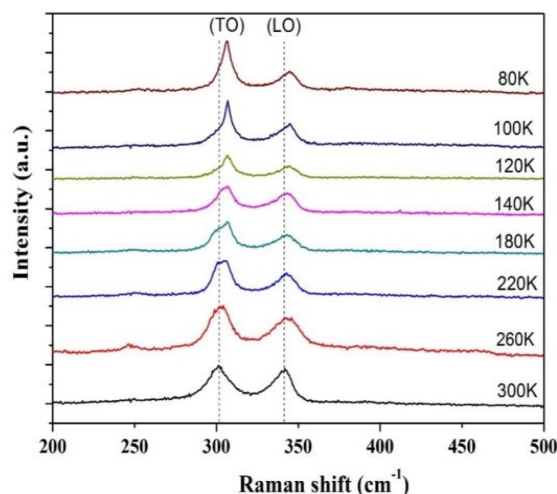


Figure 4.4 Stack plot for Raman shift

From above low temperature study of Raman shift we can determine the isobaric mode Grüneisen parameter. The Grüneisen parameter describes the effect on vibrational property of material on changing the volume, these volume changes may be a consequence of pressure or temperature change. The relation is given below for constant pressure.

$$\gamma_{iP} = - \frac{1}{\alpha \omega_i} \left(\frac{d\omega_i}{dT} \right)_P \quad (2)$$

where, α is thermal expansion coefficient, P for constant pressure. ω_i is room temperature Raman shift.

From these results the Grüneisen parameter comes out to be 1.05 for TO mode and 1.15 for LO mode as shown in **figure 4.5**

This temperature dependence can be understood in terms of anharmonic character of lattice. Literature shows that Grüneisen parameter closely follows the behavior of thermal expansion coefficient α . From the value of slope and linear thermal expansion coefficient α taken from the reported value $5 \times 10^{-6}/\text{deg.}$ and results are in good agreement with the reported value 1.44 ± 0.2 for TO mode and 1.24 ± 0.2 for LO mode [10].

Figure 4.5 Raman shift Vs. temperature

4.4 Electrical properties

4.4.1 Resistivity: The resistivity of InP crystal was measured with increasing temperature from room temperature to 500 C°. From the measured value of resistance R, thickness of the sample L and area A, we determined the resistivity ρ given as [11].

$$\rho = R \frac{A}{L} \quad (3)$$

The area of the sample is measured approximately as 0.4 cm^2 .

From the plot of resistivity vs. temperature as given in **figure 4.6**, it can be seen that resistivity decreases as the temperature increases showing semiconducting behavior of the crystal.

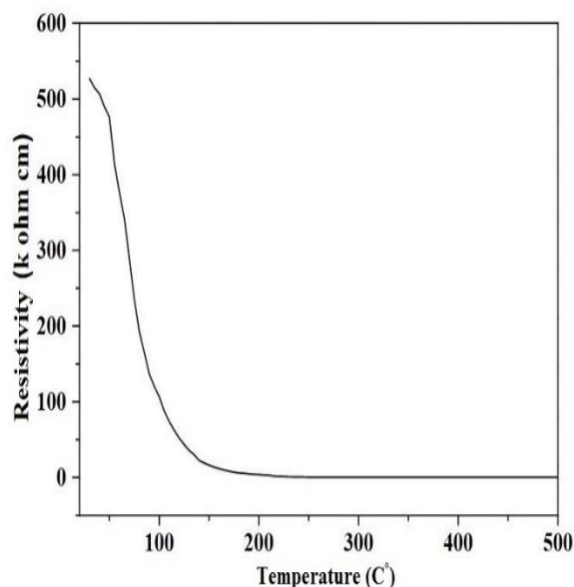
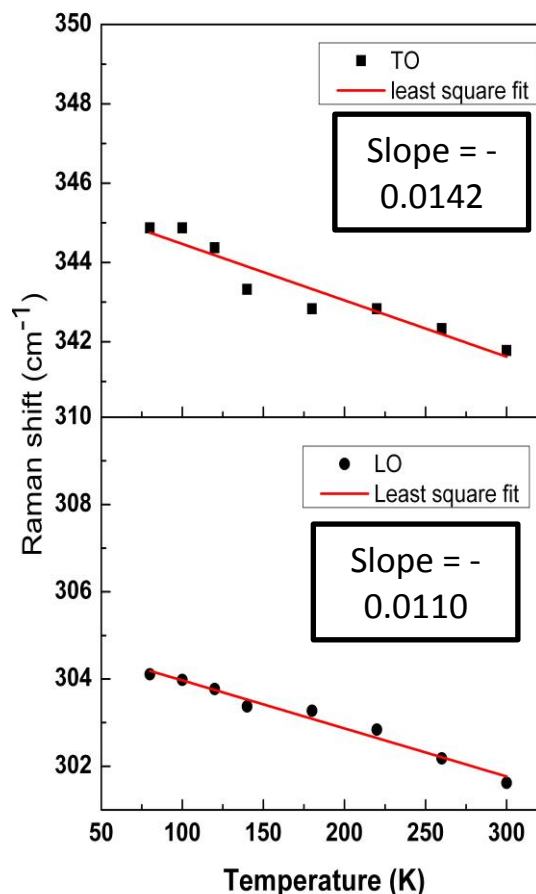


Figure 4.6 Plot of Resistivity vs. Temperature

We measure the room temperature resistivity as $5.2 \times 10^5 \Omega \text{ cm}$ which is found little less

compared to the reported value $1.0 \times 10^7 \Omega \text{ cm}$ [12].

4.4.2 Hall-effect measurement: The results were measured keeping constant magnetic field 1000 gauss and 1500 gauss, then varying the probe current, Hall voltages are measured. The value of carrier concentration comes out to be $3.2 \times 10^{14} \text{ cm}^{-3}$ and InP crystals shows n-type behavior [13].

4.4.3 Seebeck Coefficient: The Seebeck coefficient measured with increasing temperature is shown in figure 4.7. From the slope of the ΔV vs. ΔT the Seebeck coefficient obtained and comes out to be $S = -232 \mu\text{V}/^\circ\text{C}$.

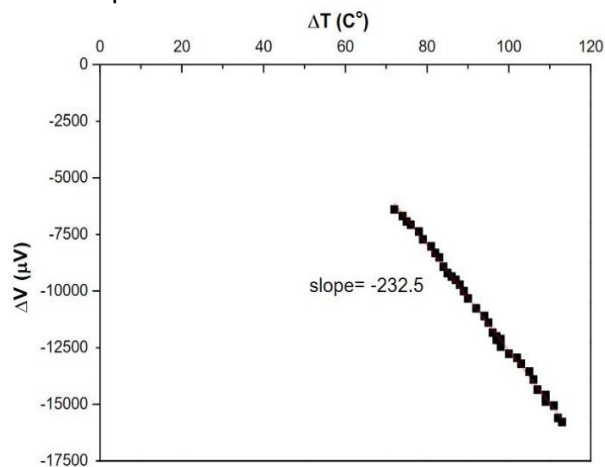


Figure 4.7 Plot of ΔV vs. ΔT

This value is almost half from the reported value of $-594 \mu\text{V}/^\circ\text{C}$ [14].

4.5 Thermal Property

4.5.1 Thermal conductivity: Thermal conductivity of InP crystal was measured by divided bar method. It is better to choose the voltage such that the ambient temperature is about 80°C . Temperatures of four thermocouples are read of periodically until two or three successive readings do not show any change indicating steady state conditions. The crystal thickness and the distances of the thermocouples from the lower end and the gradient are calculated. The coefficient of thermal conductivity for the crystal is then calculated as

$0.63 \text{ W/cm } ^\circ\text{C}$ and matches well with the reported results at 300K [15].

4.6 CONCLUSION

Grown single crystal of InP by LEC method was used in present work. EDAX analysis confirms the purity of grown InP crystal.

The X-ray diffraction confirmed that the InP crystal has Zinc blende face centered cubic structure. The XRD pattern was well indexed and the calculated lattice parameter comes out to be 5.860 \AA , which is in good agreement with the reported literature and JCPDS card. The absorption spectra show significant absorption peak at 840 nm with band gap equal to 1.46 eV. The Raman spectra shows presence of TO mode at 300.2 cm^{-1} and LO mode at 339.1 cm^{-1} at room temperature. Further, the measurement at liquid nitrogen (80 K) temperature shows TO at 306.81 cm^{-1} and LO at 344.87 cm^{-1} . The room temperature resistivity comes out to be $5.2 \times 10^5 \Omega \text{ cm}$ and as the temperature increases resistivity decreases.

The calculated thermal conductivity of InP crystals comes out to be $K_c = 0.63 \text{ W/cm } ^\circ\text{C}$ at 353K. Hall Effect measurement shows carrier concentration in InP crystal as $n = 3.2 \times 10^{14} \text{ cm}^{-3}$. Seebeck coefficient determined is $S = -232.5 \mu\text{V}/^\circ\text{C}$. Both these results show n-type nature of the InP crystal.

ACKNOWLEDGEMENTS

We are thankful to SICART (Sophisticated Instrumentation Centre for Applied Research and Technology) for EDAX and UV-VIS-NIR characterization of our sample. We are also Thankful to Dr. Vasant Sathe from IUC- DAE, Indore for helping in characterizing my samples by Raman spectroscopy at low temperature.

REFERENCES

- [1] Fang, D., Wang, X., Xu, Y. and Tan, L. (2006) Growth and properties of InP single crystals. J. of crystal growth, **66**: 327-332.

- [2] D Srideshmukhand, D. and Subhadra, K. Thermal conductivity of solids. Experiments in solid state physics. pp. 74-80.
- [3] Chen, F., Cooley, J., Hulst, W. and Smith, J. (2001) Low frequency AC measurement of the Seebeck coefficient. Review of scientific instruments, **72**: 4201-4206.
- [4] Ramamoorthy, K., Sanjeevirajaa, C., Jayachandran, M., Sankaranarayanan, K., Bhattacharya, P., Kukreja, L. (2001) Preparation and characterization of ZnO thin films on InP by laser-molecular beam epitaxy technique for solar cells. J. of crystal growth **226**: 281-286.
- [5] Deshpande, M., Patel, K. N., Gujarati, V., Patel, K., Chaki, S. Structural, thermal and optical properties of Nickel Oxide (NiO) Nanoparticles Synthesized by Chemical Precipitation Method (2016) Advanced Materials Research 1141: 65-71.
- [6] Helm, U., Roder, O., Queisser H. and Pilkuhn, M. (1970) Photoluminescence of InP. J. of Luminescence **1-2**: 542-551.
- [7] Mooradian, A. and Wright, G., (1966) First order Raman effect in III-V compound. Solid State Communi. **4**: 4-434.
- [8] Pinczuk, A., Ballman, A., Nahory, R., M. A. Pollack, M., and Worlock., J., (1979) Raman scattering studies of surface charge layers and Schottky barrier formulation in InP. J. of Vacuum Science & Technology **16**: 1168.
- [9] Hinrichs, K., Schierhorn, A., Haier, P., Esser, N., Richter, W., and Sahm, J. (1997) Phys. Rev. Lett. **79**:961.
- [10] Soma, T., Satoh, J. and Matsuo, H., (1982) Thermal expansion coefficient of GaAs and InP. Solid State Communi. **12**: 889-892.
- [11] Zhenhua, Z. and Ctirad, U. (2005) Apparatus for Seebeck coefficient and electrical resistivity measurements of bulk thermoelectric materials at high temperature. Rev. of scientific instruments **76**: 023901.
- [12] Kainosho, K., Shimakura, H., Yamamoto, H. And Oda, O. (1991) Undoped semi insulating InP by high pressure annealing. Appl. Phys. Lett. **59**: 932.
- [13] Leloup, J., Djerassi, H. and Albany J. Jordan, (1978) Hall effect in n-type InP crystals: Thermal activation. Energy and influence of compensation. J. Appl. Phys **49**: 3359-3362
- [14] Kudman, I. and Steigmeier, E. (1964) Thermal conductivity and Seebeck coefficient of InP. Phys. Rev. Lett. **133**: A1666.
- [15] Jordan A. (1985) Some thermal and mechanical properties of InP essential to crystal modeling. J. of crystal growth **71**: 559-565.